



Published in final edited form as:

*Polym Rev (Phila Pa)*. 2018 ; 58(4): 668–687. doi:10.1080/15583724.2018.1484761.

## Bio-Based Polymers for 3D Printing of Bioscaffolds

Elisa Yang<sup>a,#</sup>, Shida Miao<sup>a,#</sup>, Jing Zhong<sup>b</sup>, Zhiyong Zhang<sup>c</sup>, David K. Mills<sup>d</sup>, and Lijie Grace Zhang<sup>\*,a,e,f</sup>

<sup>a</sup>Department of Mechanical and Aerospace Engineering, The George Washington University, Washington DC 20052, USA.

<sup>b</sup>The University of Akron, Akron, 44304, USA.

<sup>c</sup>Translational Research Centre of Regenerative Medicine and 3D Printing Technologies of Guangzhou Medical University, The Third Affiliated Hospital of Guangzhou Medical University, Guangzhou City, Guangdong Province, 510150, PR China.

<sup>d</sup>School of Biological Sciences and the Center for Biomedical Engineering & Rehabilitation Science. Louisiana Tech University, Ruston, LA 71272, USA

<sup>e</sup>Department of Biomedical Engineering, The George Washington University, Washington DC 20052, USA.

<sup>f</sup>Department of Medicine, The George Washington University, Washington DC 20052, USA.

### Abstract

Three-dimensional (3D) printing technologies enable not only faster bioconstructs development but also on-demand and customized manufacturing, offering patients a personalized biomedical solution. This emerging technique has a great potential for fabricating bioscaffolds with complex architectures and geometries and specifically tailored for use in regenerative medicine. The next major innovation in this area will be the development of biocompatible and histiogenic 3D printing materials with bio-based printable polymers. This review will briefly discuss 3D printing techniques and their current limitations, with a focus on novel bio-based polymers as 3D printing feedstock for clinical medicine and tissue regeneration.

### Keywords

3D printing; Bio-based polymer; Cellulose; PHA; Soybean oil; Soy protein

## 1. Introduction

3D printing, also known as additive manufacturing (AM), is the process of layering material to construct a three-dimensional structure with high precision from a computer aided design (CAD).<sup>1–3</sup> Complex 3D products, with precisely controlled architecture (external shape,

\*Corresponding author: Dr. Lijie Grace Zhang, Tel: 202-994-2479, Fax: 202-994-0238, lgzhang@gwu.edu, Mailing Address: 800 22nd Street NW Science and Engineering Hall, Room 3590, Washington DC, 20052.

#Elisa Yang and Shida Miao contributed equally to this manuscript. Elisa is a research assistant in Prof. Zhang's group. Shida is a postdoctoral scientist working on 3D&4D printing of bio-based polymers.

internal pore geometry, and interconnectivity), have been fabricated using 3D printing with high reproducibility and repeatability.<sup>4–8</sup> In view of the versatility of 3D printing, it has been promoted as the initiation of a new industrial revolution.<sup>9, 10</sup> 3D printing of bioscaffolds refers to the printing of bioscaffolds with biocompatible and bioresorbable materials to construct a 3D structure comparable to the implant tissue area and designed to promote tissue integration and regeneration and enhance injury recovery. The global market of 3D printing of bioproducts is expected to grow into a \$1.82 billion market by 2022, which includes bio-based products and materials for analytical, dental, medical, orthopedic, consumer testing, and food applications.<sup>11, 12</sup> Along with the rapid growth of 3D printing of bioscaffolds, corresponding printable materials are in growing demand and have become one of the most intensely research areas over the past five years.<sup>12–15</sup>

Bio-based polymers are bio-products derived from living organisms such as plants, trees and algae.<sup>16–18</sup> As the industry of bioplastics grows, the terms “bio-based” and “biodegradable” are used interchangeably, but, in this review, we wish to make a clear distinction between these two polymer types.<sup>19–22</sup> A biodegradable material is one that can be degraded naturally by micro-organisms, whereas a bio-based material is derived from agricultural resources such as corn or soybeans.<sup>19–22</sup> Bioplastics can be biodegradable, bio-based, or a combination of both. However, a bio-based material does not guarantee biodegradability. Environmental concerns have stimulated research efforts to explore the process of creating bio-based materials and their applications.<sup>23–26</sup> For instance, pyrolysis, hydrolytic cracking, and fermentation processes are common industrial methods used to extract sugars, starches, oils, etc. from crops.<sup>27–32</sup> These intermediate products can then be converted into bio-based plastics such as poly lactic acid (PLA), polyhydroxyalkanoates (PHAs), and cellulose degenerates.

Considering the significant knowledge produced on bio-based polymers and their inherent properties, exploration of printing materials from bio-based polymers is an innovative idea that has attracted worldwide interest.<sup>33–36</sup> For example, 3D macroporous gelatin methacrylamide constructs were fabricated by combining insight gained from material chemistry, engineering, and biology to achieve high cell viability (>97%)<sup>37</sup>; high-density collagen hydrogels were used to print tissue constructs which were mechanically stable and able to support and maintain cell growth.<sup>38</sup>

In this review, we will briefly discuss the approaches to 3D printing of bioscaffolds and current techniques and subsequently comment on the future potential of bio-based materials for 3D printing of bioscaffolds, with emphasis on cellulose-derived polymers, PLA, PHAs, soybean oil based polymers, and soybean protein. Natural hydrogel polymers including alginate, gelatin, collagen, chitosan, fibrin and hyaluronic acid are extensively applied as 3D printing materials and readers are directed to these excellent reviews.<sup>12, 39–42</sup>

## 2. 3D printing technologies and applications

3D printing technology is widely used for a variety of applications and many techniques such as material extrusion, powder bed fusion, and vat photopolymerization have already been developed.<sup>14, 43–47</sup> For 3D printing of bioscaffolds with bio-based polymers,

stereolithography (SL), fused deposition modeling (FDM) and binder jetting are frequently used methods.<sup>7, 14, 48–66</sup> These 3D printing technologies are compared in Table 1 and are briefly discussed below.

Since its discovery in the early 1970s, stereolithography (SL) has become one of the most common 3D printing techniques.<sup>54, 67</sup> The process consists of a container with a liquid photopolymerizable resin and an ultraviolet (UV) laser held by galvanometers. Directed by a CAD program, the laser beam traces a design onto the resin creating a hardened layer. The steps are repeated with new resin layers until the design is completed. A similar process known as digital light processing (DLP), also utilizes UV light but with a projector below the resin, so that all layers can be exposed at once. With DLP, the size of the structure can present limitations but compared to SL, fewer fabrication steps are required, which offers a faster print time.<sup>68–70</sup> The laser used in SL is capable of producing smaller cross-sectional areas, allowing detailed designs with a resolution range of 150  $\mu\text{m}$ .<sup>71</sup> The disadvantage of SL is that the laser unit is expensive. The cost of the machines is always negligible when compared to human health and life. Thus, SL is still highly desirable and promising for development of bioscaffolds.

Fused deposition modeling (FDM) utilizes extrusion to print 3D structures.<sup>56, 72, 73</sup> The 3D printer uses heat to extrude layers of a thermoplastic material, commonly acrylonitrile butadiene styrene (ABS) or poly lactic acid (PLA), from a nozzle onto a base.<sup>56, 73, 74</sup> The deposited layers fuse together and harden into the final construct. Advantages of this method are durability, high accuracy, and low material cost.<sup>58, 75–77</sup> Furthermore, its precision allows printing of complex scaffolds for numerous engineering applications. Compared to SL, the limitation of FDM is that the printed objects always have contour-like surficial structures caused by filament-fused-deposition manufacturing, which has impeded the acquisition of smooth surfaces.<sup>78</sup>

Binder jetting or inkjet printing is the process of creating layers using bonding powder and a binding material.<sup>79, 80</sup> Each layer starts with a thin layer of powder on top of the platform. A movable inkjet unit distributes a binder material that selectively joins particles based on the corresponding CAD model. The process is repeated with new layers until the structure is complete. A post-production process uses heat to remove any unbound powder remaining. While binder jetting advantageously features rapid printing speed and low costs, there are challenges with post-production processes, including powder removal from printed scaffolds and reduced compressive strength due to the applied heat treatment.<sup>63</sup> In addition, a common limitation with binder jetting is relative low resolution in 3D printed constructs.

These techniques have demonstrated their capability to fabricate bioscaffolds. Gauvin and the colleagues utilized SL to create scaffolds that mimicked the microarchitecture of tissues.<sup>81</sup> In addition to the structural intricacy, the scaffolds had high porosity and were capable of uniformly distributing and proliferating human umbilical vein endothelial cells. Chen et al. applied FDM to produce polycaprolactone scaffolds for bone tissue applications.<sup>82</sup> With the addition of a matrix consisting of hyaluronic acid, methylated collagen and terpolymer, their scaffolds exhibited high cell seeding efficiency and osteogenic differentiation. Zein et al. used FDM to create poly( $\epsilon$ -caprolactone) scaffolds with an innovative honeycomb

architecture.<sup>72</sup> Each layer extruded measured 0.254 mm thick. The morphology of the 3D structures expressed fully interconnected channel networks with controlled porosity. Multi-cell constructs consisting of human amniotic fluid derived stem cells, canine smooth muscle cells, and bovine aortic endothelial cells were printed by Xu and the colleagues, demonstrating the ability to produce complex tissue constructs with binder jetting.<sup>83</sup> These studies provide a strong basis for 3D printing bioscaffolds with bio-based polymers.

### 3. Bio-based polymers for 3D printing of bioscaffolds

#### 3.1 Cellulose-derived polymers

The abundant availability of cellulose has made this organic polymer an attractive material for use in 3D printing of bioscaffolds. Cellulose-based polymers are widely used in pill fabrication.<sup>84</sup> Cellulose acetate and hydroxypropyl methylcellulose were 3D printed to manufacture a multi-active solid dosage form known as polypill.<sup>85</sup> A hydrophobic cellulose acetate shell was first extruded; active drugs were mixed with hydrophilic hydroxypropyl methylcellulose and extruded into the segmented compartments of cellulose acetate to form sustained release compartments. This polypill demonstrates that complex medication regimes can be combined into a single customized tablet, which could potentially improve adherence for patients currently taking multiple tablets and allow personalization of a particular drug combination/drug release to fit the needs of an individual.

Nanocellulose has been used to 3D print wound dressing materials because it offers strength, produces a transparent film, creates a moist wound healing environment, and forms elastic gels with bioresponsive characteristics.<sup>86</sup> Two different nanocelluloses were prepared with (2,2,6,6-tetramethyl-piperidin-1-yl)oxyl (TEMPO) mediated oxidation and a combination of carboxymethylation and periodate oxidation. The latter resulted in a homogeneous material with short nanofibrils of widths less than 20 nm and lengths less than 200 nm. Due to the small dimensions of the nanofibrils, good rheological properties were achieved for use as a 3D printing bioink. The printed 3D porous structures were found to suppress bacterial growth, an interesting property for a wound dressing application.

Markstedt et. al. combined nanofibrillated cellulose with alginate to print cartilage tissues.<sup>36</sup> The shear thinning properties of cellulose yielded 2D and 3D shaped structures. Interestingly, using magnetic resonance imaging (MRI) and computed tomography (CT) images as blueprints, anatomically shaped cartilage structures, such as a human ear and sheep meniscus, were 3D printed as shown in Figure 1. The cellulose-alginate blend was capable of printing at room temperature with a low pressure. Furthermore, the printed structures were biocompatible and cell supportive (Figure 1). Cell viability was 73% and 86% after 1 and 7 days, respectively, in human chondrocytes which were printed with the noncytotoxic, nanocellulose-based material. Although developing printable materials with natural cellulose polymers to print 3D structures is still an evolving technique in tissue engineering, this study provides a glimpse of the potential of nanocellulose being used for 3D printing of living tissues.

### 3.2 Polylactic acid (PLA)

Polylactic acid (PLA) is a polyester derived from renewable resources like corn starch and sugar beets.<sup>87, 88</sup> In addition to its fast biodegradability, the material is relatively cheap, easily produced, and can produce constructs of high resolution in 3D printing.<sup>89</sup> PLA is one of the most popular materials in research and industry because it has a low crystallization rate, high dimensional stability as well as tunable properties by adding pigments, nucleating agents, UV stabilizers, and inorganic particles, allowing for many applications such as wounds materials, tissue regeneration, bone defects, and controlled drug delivery.<sup>90–93</sup>

PLA has been used widely to 3D print a variety of geometries, as shown in Figure 2.<sup>89, 94</sup> The scaffold geometry including pores size, shape, struts size, and orientation significantly affects mechanical performance, permeability, nutrient access, diffusion and cell response.<sup>95</sup> For example, mesenchymal stem cell (MSC) differentiation and proliferation of pre-osteoblastic cells were highly affected by the geometry of individual pores within the scaffold.<sup>96, 97</sup> Nonetheless, 3D printed PLA scaffolds with different architectures are investigated for biomedical applications in view of their good biocompatibility and biodegradation. Almeida and the colleagues explored the application of PLA scaffolds for inflammation in tissue repair.<sup>98</sup> Using nozzle deposition, they created orthogonal scaffolds with pores of  $165 \pm 5 \mu\text{m}$  in the axial direction and struts  $75 \pm 5 \mu\text{m}$ . The scaffolds were then seeded with human monocytes and the results showcased high production of interleukin. Kao and the colleagues printed PLA scaffolds coated with polydopamine and seeded with human adipose-derived stem cells.<sup>99</sup> The coating enabled enhanced adhesion and proliferation. Their results also increased collagen I secretion and cell cycle progression, providing sufficient support in the use of PLA to direct cell responses in bone tissue engineering. Another study by Rosenzweig et al. demonstrated the use of PLA scaffolds for cartilage and nucleus pulposus tissue regeneration.<sup>100</sup> Articular chondrocytes and nucleus pulposus cells were cultured. After three weeks, high levels of cell viability, proteoglycan, and collagen II were detected.

Using supporting structures made with PLA, hierarchical multiphase scaffolds can be fabricated, offering complex and multifunctional tissue regeneration. A biphasic (PLA/gelatin) vascularized bone construct was developed by a dual 3D bioprinting platform technique.<sup>101</sup> PLA fiber was fabricated into a hard bone scaffold using an FDM printer, while gelatin methacrylate hydrogel was printed into an elastic blood vessel using SL printing. In the integrative design, complex vascularized bone constructs, comprised of a hard-mineral structure surrounded by a soft organic matrix, were able to more closely mimic natural bone characteristics. Moreover, they also introduced the regional immobilization of bioactive factors into construct design to promote osteogenesis and angiogenesis through biocompatible mussel inspired adhesion and “thiol-ene” click reactions.

While FDM has the capacity to fabricate PLA into various architectures, the high temperature required for FDM fabrication makes it difficult to successfully incorporate bioactive components into scaffolds or include bioactive growth factors; although FDM has been used to print drug doped medical devices including catheters, pessaries, filaments, bone screws, and stents for cleft lip repair, FDM still has difficulties in achieving biomimetic nano resolution for regulating cellular events.<sup>93</sup> A recent work used surface modification to

improve biocompatibility and functionality of 3D printed PLA scaffolds, providing significantly greater potential for biomedical application.<sup>102</sup> The bone scaffolds were printed using PLA with an FDM printer. A novel and simple surface modification strategy was implemented to control the release of bioactive factors in a spatiotemporal manner through a layer-by-layer (gelatin/polylysine) assembly technique. This provided a nanoscale surface and allowed immobilizing bioactive cues to be put onto the biomimetic 3D scaffolds. As shown in Figure 3, compared to an unmodified PLA control, both human mesenchymal stem cells (hMSCs) and human umbilical vein cells (HUVECs), on the 3D bioprinted scaffolds modified with nanocoating, exhibited excellent adhesion and proliferation. hMSCs were widely distributed and maintained a spindle morphology while HUVECs preferred to grow in lines and form an highly aligned network-like structure (Figure 3 C).

Besides acting as a backbone for scaffolds, PLA can be used to develop complex structures with minimal material loss. For example, PLA was used to print a 3D mold; thermoset resin was then poured into the mold.<sup>103</sup> After a curing process, PLA was readily removed by immersion in chloroform while the cross-linked thermoset structures, with controlled and graded porosity, were leftover.<sup>103</sup> The graded structure mimics the non-uniform distribution of porosity found within natural tissues (Figure 4). This guided approach using a mold exhibited different pore morphologies, creating enhanced biomedical conditions.<sup>103</sup>

### 3.3 Polyhydroxyalkanoates (PHAs)

Polyhydroxyalkanoates (PHAs) are natural polymers made by bacterial fermentation.<sup>104–106</sup> PHAs offer the benefits of being biodegradable, high biocompatibility, and are available from renewable resources.<sup>104–106</sup> Common applications in the market currently include implant/surgical products, medical and food packaging, and stem cell growth. Within PHAs, there are a variety of derived materials used in research including polyhydroxybutyrate (PHB), poly(3-hydroxybutyrate-co-3-hydroxyvalerate) (PHBV), and poly-4-hydroxybutyrate (P4HB).<sup>104–106</sup> Similarly to PLA, this material can be modified through temperature, enzymes, and inorganic materials to improve its mechanical properties and chemical functionalities. Wu et al. improved the hydrophilicity of PHBV scaffolds by adding bioactive glass (BG).<sup>107</sup> The hybrid scaffolds were seeded with rabbit articular chondrocytes and exhibited good cell migration, an increased adhesion and proliferation percentage, and greater extracellular matrix content. Additionally, BG increased the mechanical strength of the scaffold. These results indicate the possibility of using PHBV modified scaffolds for bone repair and cartilage tissue engineering.

Typically, with PHAs, techniques like solvent casting, leaching, gas foaming, and electrospinning are used to make polymeric scaffolds. Xing and others conducted a study to assess PHBV scaffolds for *in vitro* antibacterial activity against *Staphylococcus aureus* and *Klebsiella pneumoniae*.<sup>108</sup> Using electrospinning, they created nanofibrous scaffolds loaded with metallic silver particles. While the PHBV scaffolds alone did not greatly improve antibacterial activity, the addition of silver to PHBV showed 90% bacterial growth inhibition or greater. Most importantly, the PHBV scaffolds had good cell compatibility and viability, supporting the potential for joint replacement applications. PHAs have also been studied for nerve tissue regeneration. Prabhakaran and the colleagues fabricated composite scaffolds

made of PHBV and collagen to study biocompatibility and neurite outgrowth.<sup>109</sup> Compared to random patterns, the aligned nanofibrous scaffolds showed superior cell differentiation. Also, neurite elongation grew parallel to the direction of orientation of the nanofibers. Masaeli and others had similar results for their PHBV/collagen I scaffolds where cell proliferation was significantly higher on aligned fibers.<sup>110</sup> Their research concluded that for aligned fibrous scaffolds, the cells oriented in the direction of fiber alignment due to contact guidance phenomenon. These findings suggest that PHBV scaffolds can be successfully used for nerve grafts in neural engineering with the appropriate fiber orientation and blended compositions.

Using FDM printing with PHA filaments is another emerging candidate for 3D bioprinting. By carefully examining the temperature control elements of extrusion machines as well as the thermal properties of the PHA material, usable PHA filaments were fabricated with suitable extrusion speed and post-extrusion processes. However many research efforts with PHA have faced difficulty forming filament materials.<sup>111, 112</sup> Some factors may be responsible for the delay in 3D printing of PHA scaffolds. Unlike common 3D printing materials such as ABS and PLA, PHA has a smaller production scale, making it less interesting to 3D printing industries. Although 3D printing was invented decades ago, it is still an advancing technology with a young market, and researchers in PHA study have not extensively expanded their studies in 3D printing fields. However, due to their excellent biocompatibility and biodegradation properties, future efforts to develop PHA based 3D scaffolds are highly anticipated.

### 3.4 Soybean oil based polymers

Soybean oils are a valuable feedstock used in preparation of a variety of polymers including polyurethane, polyester, polyether and polyolefin.<sup>16, 113–115</sup> Although soybean oils are not naturally present as polymers, they are precursors for monomer chains that can be used to synthesize various polymers, making the polymers' structures changeable by converting soybean oil to different monomers.<sup>16</sup> Soybean oil based monomers have a similar structure as petroleum-based monomers, making them alternatives for petroleum-based biopolymers.<sup>16</sup>

Soybean oil can be easily prepared at room temperature and manipulated for the desired physical properties. For example, when Hong and Wool combined soybean oil with keratin fibers, they observed an increase in storage modulus, resistance to fracture, and bend strength.<sup>116</sup> Kolanthai et. al. prepared and tested copolyesters made of soybean oil cross linked with sebacic and citric acid.<sup>117</sup> After the scaffolds were prepared using the methods of salt leaching and freeze drying, bone marrow hMSCs were seeded. Despite no osteoinductive factors being added, on day 7 calcium phosphate deposits formed, indicating osteogenic differentiation. By day 14, there was a significant increase in mineral deposits. These results show possible applications of soybean oil in bone tissue engineering. Sitterger and the colleagues implanted soybean scaffolds in mice to determine *in vivo* biocompatibility.<sup>118</sup> Two scaffolds, soy-gelatin blend and soy-alginate blend were tested. Overall, the soy-gelatin blend had a higher clindamycin percentage of release compared to the soy-alginate blend, most likely due to the pore structure and faster degradation rate.

However, both scaffolds managed to significantly decrease the viability of bacteria compared to the non-releasing control scaffolds. This presents a novel, low-cost alternative to current medical applications particularly in skin and cartilage that use synthetic materials which often increase the likelihood of infection and are unable to degrade.

Soybean oil epoxidized acrylate has been used as photocurable liquid resin to fabricate biocompatible scaffolds.<sup>119</sup> As shown in Figure 5, smart and highly biocompatible scaffolds capable of supporting growth of multipotent human bone marrow mesenchymal stem cells (hMSCs) were developed through 3D stereolithography printing. The porosity of the scaffolds was readily adjusted by changing printing infill density. Laser frequency and printing speed significantly affected superficial structures of the polymerized soybean oil epoxidized acrylate. Remarkably, the shape memory scaffolds formed a temporary shape at  $-18\text{ }^{\circ}\text{C}$  and fully recovered their original shape at human body temperature ( $37\text{ }^{\circ}\text{C}$ ), which indicates the great potential for 4D printing applications. More importantly, the soybean oil materials showed similar cell compatibility with PLA and polycaprolactone (PCL), significantly higher than with polyethylene glycol diacrylate (PEGDA).

### 3.5 Soy Protein

Soy protein is a versatile bio-based material already widely used in the food industry as a renewable alternative to plastics.<sup>120, 121</sup> Novel endeavors in soy protein as a new biomaterial have continually increased as a result of its low cost and ready availability. Additional advantages of soy protein compared to other natural proteins are its long shelf life and plant origins.<sup>122</sup> Furthermore, it can be mixed with other materials to yield different chemical and mechanical properties. Soy protein has shown great potential in the field of 3D printing tissue scaffolds.<sup>123</sup>

Bone defects and surgical treatments require implants to support the growth of new tissues. Low immunogenicity and tissue regeneration are important to the implantation of biomaterials. Soybean contains isoflavones known to alleviate tumor cell proliferation and slow down immunocompetent cell activity. Santin and the colleagues studied the effects of a bone filler derived from soybean curd on osteoblast cell behavior.<sup>124</sup> The new biomaterial was made by thermosetting defatted soybean curd. They found that the fillers reduced osteoblast proliferation and stimulated an increase in collagen when inserted *in vitro*. The material could be used to make films, porous scaffolds, and granules. The promising results show potential to use soybean fillers to reduce the inflammatory response of macrophages induced by implants as well as delay bone resorption.

A study by Chien et. al. studied the effects of soy protein for *in vivo* inserted implants.<sup>125</sup> Soy protein scaffolds degraded in 14 days whereas bovine collagen (FDA-approved) scaffolds took much longer, 56 days, to degrade. To examine the effects of the soy scaffolds on immune response, different levels of protein were loaded. Lower soy protein weight in the scaffold did not produce as much inflammation as the scaffold with a higher protein weight. Furthermore, the scaffold with more protein, less porosity, and slower degradation had a more severe immune response. Over time, soy-specific antibodies were formed after scaffold implantation but no allergies were detected. In addition to protein density, scaffold degradation and porosity play important roles. Chien and Shah modified soy protein with



heat and enzyme crosslinking to create scaffolds.<sup>126</sup> The enzyme treatment increased degradation time by 1 week and increased hMSC viability. Potentially, soy protein scaffolds can be successfully integrated into regenerative medicine when optimal protein density and controlled scaffold degradation are fully understood.

Soy protein also has interesting capabilities for drug delivery and wound healing applications. While the physical properties in its purest form are not optimal, other natural polymers can be blended with soy protein to increase its biostability. Olami and others made a blended structure consisting of soy protein and alginate to examine the release profile of the drug clindamycin.<sup>127</sup> The drug release had a burst effect of 70% and decreased in release rate for 4 days. Corresponding to the release, there was a significant diminution in bacterial viability. Peles and the colleagues found similar success by creating a soy protein isolate matrix injected with gentamicin.<sup>128</sup> The release profile was moderate with a decreased release rate for 4 weeks. These results using soy protein clearly validate their possibility for drug and cell carrier platforms.

One difficulty working with soy protein is creating a scaffold with fine fibrous structures. Most proteins have weak water stability and creating fibers are difficult. Xu and the colleagues developed water stable scaffolds without crosslinking by creating a slurry of soy protein, 10 wt% cysteine, and sodium dodecyl sulfate.<sup>129</sup> Adipose derived mesenchymal stem cells were seeded onto the ultrafine fibrous scaffolds. After incubation in PBS for 28 days, the scaffolds preserved their fibrous structures, indicating superior tolerance compared to other researched 3D soy protein scaffolds (with and without crosslinking). In addition, after 2 weeks of cell culture, the 3D electrospun scaffolds had 227% and 114% higher cell proliferation than the 2D scaffolds and 3D commercial scaffolds had. This can be attributed to the fact that the fibers in the 2D scaffolds were more tightly stored, limiting cell penetration whereas the 3D scaffolds were more porous. The 3D commercial scaffolds presented deeper cell penetration but the cell distribution was not uniform as the cells only attached to the walls of the scaffold. Comparing cell differentiation, the 3D scaffolds had the highest increase in newly secreted fat supporting 3D soy protein-based scaffolds as an alternative solution in tissue engineering applications to address volume loss or tissue replacement due to trauma.

As a relatively new bioprinting material, soy protein has shown auspicious results in the 3D printing field. Chien et al. designed a study to use denatured soy protein and bioplotting to create specific 3D constructs.<sup>130</sup> A soy protein slurry was prepared and inserted into a polyethylene syringe, then extruded through a 3D Bioplotter. To print scaffolds with controlled pore geometry, slurries consisting of various concentrations of soy protein and glycerol, to decrease mass flow rate, were used. To increase mass flow rate, the extrusion pressure was increased to a limit of 0.0072+/-0.0002 g/s. Any lower or higher pressure produced indistinct constructs. The scaffolds were cured with ethanol then treated with dehydrothermal (DHT), freeze drying and DHT, and chemical crosslinking with 1-ethyl-3-(3-dimethylaminopropyl) carbodiimide (EDC). Figure 6 shows SEM images of their surface morphology. Human mesenchymal stem cells survived on all scaffolds, with the non-treated and thermally-treated scaffolds having the highest cell attachment efficiency (Figure 6B).

#### 4. Perspective and conclusions

Bio-based polymers, including cellulose derived polymers, PLA, PHAs, soybean oil based polymers, and soy protein, are great material candidates for future 3D printing of bioscaffolds. Foundational research efforts show promise in bio-based materials to replace traditional printing materials such as petroleum derived plastics.

Printing strategies and novel material designs play important roles in the fabrication of bioscaffolds. Although initial efforts to adjust printing systems to produce desirable structures with bio-based materials have been made, there are still challenges to fabricate advanced and fully functionalized tissues/medicines. Thus, exploring new structural bio-based polymers and chemically modifying current bio-based polymers to enhance their biocompatible and printable features will be vital for achieving clinical bioscaffolds with bio-based polymers in the future. Understanding *in vitro/vivo* interactions with bio-based polymers while maintaining their printing integrity is another subsequent step for advancement. 3D printing of bioscaffolds with bio-based polymers is an emerging field and its exponential development is foreseeable in the near future.

#### Acknowledgements:

The authors would like to thank the NIH Director's New Innovator Award, 1DP2EB020549-01, NSF BME program grant # 1510561, and NSF MME program grant # 1642186 for financial support.

#### References:

1. Ambrosi A; Pumera M, "3D-printing technologies for electrochemical applications", *Chem. Soc. Rev* 2016, 45, 2740–2755. [PubMed: 27048921]
2. Minas C; Carnelli D; Tervoort E; Studart AR, "3D Printing of Emulsions and Foams into Hierarchical Porous Ceramics", *Adv. Mater* 2016, 28, 9993–9999. [PubMed: 27677912]
3. Muth JT; Vogt DM; Truby RL; Mengüç Y; Kolesky DB; Wood RJ; Lewis JA, "Embedded 3D printing of strain sensors within highly stretchable elastomers", *Adv. Mater* 2014, 26, 6307–6312. [PubMed: 24934143]
4. Kalsoom U; Nesterenko PN; Paull B, "Recent developments in 3D printable composite materials", *RSC Adv.* 2016, 6, 60355–60371.
5. Mannoor MS; Jiang Z; James T; Kong YL; Malatesta KA; Soboyejo WO; Verma N; Gracias DH; McAlpine MC, "3D printed bionic ears", *Nano Lett.* 2013, 13, 2634–2639. [PubMed: 23635097]
6. Hong S; Sycks D; Chan HF; Lin S; Lopez GP; Guilak F; Leong KW; Zhao X, "3D printing of highly stretchable and tough hydrogels into complex, cellularized structures", *Adv. Mater* 2015, 27, 4035–4040. [PubMed: 26033288]
7. Zhang AP; Qu X; Soman P; Hribar KC; Lee JW; Chen S; He S, "Rapid fabrication of complex 3D extracellular microenvironments by dynamic optical projection stereolithography", *Adv. Mater* 2012, 24, 4266–4270. [PubMed: 22786787]
8. Pati F; Jang J; Ha D-H; Kim SW; Rhie J-W; Shim J-H; Kim D-H; Cho D-W, "Printing three-dimensional tissue analogues with decellularized extracellular matrix bioink", *Nat. Commun* 2014, 5.
9. Weller C; Kleer R; Piller FT, "Economic implications of 3D printing: Market structure models in light of additive manufacturing revisited", *Int. J. Prod. Econ* 2015, 164, 43–56.
10. Berman B, "3-D printing: The new industrial revolution", *Bus. Horizons* 2012, 55, 155–162.
11. Jose RR; Rodriguez MJ; Dixon TA; Omenetto F; Kaplan DL, "Evolution of bioinks and additive manufacturing technologies for 3D bioprinting", *ACS Biomater. Sci. Eng* 2016, 2, 1662–1678.

12. Cui H; Nowicki M; Fisher JP; Zhang LG, “3D Bioprinting for Organ Regeneration”, *Adv. Healthc. Mater* 2016.
13. Miao S; Castro N; Nowicki M; Xia L; Cui H; Zhou X; Zhu W; Lee S.-j.; Sarkar K; Vozzi G, “4D printing of polymeric materials for tissue and organ regeneration”, *Mater. Today* 2017, 10.1016/j.mattod.2017.06.005.
14. Murphy SV; Atala A, “3D bioprinting of tissues and organs”, *Nat. Biotechnol* 2014, 32, 773–785. [PubMed: 25093879]
15. Kolesky DB; Truby RL; Gladman A; Busbee TA; Homan KA; Lewis JA, “3D bioprinting of vascularized, heterogeneous cell-laden tissue constructs”, *Adv. Mater* 2014, 26, 3124–3130. [PubMed: 24550124]
16. Miao S; Wang P; Su Z; Zhang S, “Vegetable-oil-based polymers as future polymeric biomaterials”, *Acta Biomater.* 2014, 10, 1692–1704. [PubMed: 24012607]
17. Zhang C; Garrison TF; Madbouly SA; Kessler MR, “Recent Advances in Vegetable Oil-Based Polymers and Their Composites”, *Prog. Polym. Sci* 2017.
18. D’Souza J; Camargo R; Yan N, “Biomass liquefaction and alkoxylation: A review of structural characterization methods for bio-based polyols”, *Polym. Rev* 2017, 00–00.
19. Imre B; Pukánszky B, “Compatibilization in bio-based and biodegradable polymer blends”, *Eur. Polym. J* 2013, 49, 1215–1233.
20. Hottle TA; Bilec MM; Landis AE, “Sustainability assessments of bio-based polymers”, *Polym. Degrad. Stab* 2013, 98, 1898–1907.
21. Vieira MGA; da Silva MA; dos Santos LO; Beppu MM, “Natural-based plasticizers and biopolymer films: A review”, *Eur. Polym. J* 2011, 47, 254–263.
22. Mülhaupt R, “Green polymer chemistry and bio-based plastics: dreams and reality”, *Macromol. Chem. Phys* 2013, 214, 159–174.
23. Miao S; Callow NV; Ju LK, “Ethyl rhamnolipids as a renewable source to produce biopolyurethanes”, *Eur. J. Lipid Sci. Technol* 2015, 117, 156–160.
24. Miao S; Zhang S; Su Z; Wang P, “A novel vegetable oil–lactate hybrid monomer for synthesis of high-Tg polyurethanes”, *J. Polym. Sci. A Polym. Chem* 2010, 48, 243–250.
25. Miao S; Zhang S; Su Z; Wang P, “Synthesis of bio-based polyurethanes from epoxidized soybean oil and isopropanolamine”, *J. Appl. Polym. Sci* 2013, 127, 1929–1936.
26. Miao S; Zhang S; Su Z; Wang P, “Chemoenzymatic synthesis of oleic acid-based polyesters for use as highly stable biomaterials”, *J. Polym. Sci. A Polym. Chem* 2008, 46, 4243–4248.
27. Abnisa F; Daud WMAW, “A review on co-pyrolysis of biomass: an optional technique to obtain a high-grade pyrolysis oil”, *Energy Convers. Manag* 2014, 87, 71–85.
28. Kibet JK; Khachatryan L; Dellinger B, “Phenols from pyrolysis and co-pyrolysis of tobacco biomass components”, *Chemosphere* 2015, 138, 259–265. [PubMed: 26091866]
29. Zhang J; Choi YS; Yoo CG; Kim TH; Brown RC; Shanks BH, “Cellulose–hemicellulose and cellulose–lignin interactions during fast pyrolysis”, *ACS Sustainable Chem. Eng* 2015, 3, 293–301.
30. Koutinas AA; Vlysidis A; Pleissner D; Kopsahelis N; Garcia IL; Kookos IK; Papanikolaou S; Kwan TH; Lin CSK, “Valorization of industrial waste and by-product streams via fermentation for the production of chemicals and biopolymers”, *Chem. Soc. Rev* 2014, 43, 2587–2627. [PubMed: 24424298]
31. Ray SG; Ghangrekar M, “Enhancing organic matter removal, biopolymer recovery and electricity generation from distillery wastewater by combining fungal fermentation and microbial fuel cell”, *Bioresour. Technol* 2015, 176, 8–14. [PubMed: 25460978]
32. Sukan A; Roy I; Keshavarz T, “Dual production of biopolymers from bacteria”, *Carbohydr. Polym* 2015, 126, 47–51. [PubMed: 25933521]
33. Klotz BJ; Gawlitta D; Rosenberg AJ; Malda J; Melchels FP, “Gelatin-methacryloyl hydrogels: towards biofabrication-based tissue repair”, *Trends Biotechnol.* 2016, 34, 394–407. [PubMed: 26867787]
34. Skardal A; Atala A, “Biomaterials for integration with 3-D bioprinting”, *Ann. Biomed. Eng* 2015, 43, 730–746. [PubMed: 25476164]

35. Kundu J; Shim JH; Jang J; Kim SW; Cho DW, “An additive manufacturing-based PCL–alginate–chondrocyte bioprinted scaffold for cartilage tissue engineering”, *J. Tissue Eng. Regen. Med* 2015, 9, 1286–1297. [PubMed: 23349081]
36. Markstedt K; Mantas A; Tournier I; Martínez Ávila H.c.; Hägg D; Gatenholm P, “3D bioprinting human chondrocytes with nanocellulose–alginate bioink for cartilage tissue engineering applications”, *Biomacromolecules* 2015, 16, 1489–1496. [PubMed: 25806996]
37. Billiet T; Gevaert E; De Schryver T; Cornelissen M; Dubrue P, “The 3D printing of gelatin methacrylamide cell-laden tissue-engineered constructs with high cell viability”, *Biomaterials* 2014, 35, 49–62. [PubMed: 24112804]
38. Rhee S; Puetzer JL; Mason BN; Reinhart-King CA; Bonassar LJ, “3D bioprinting of spatially heterogeneous collagen constructs for cartilage tissue engineering”, *ACS Biomater. Sci. Eng* 2016, 2, 1800–1805.
39. Stanton M; Samitier J; Sánchez S, “Bioprinting of 3D hydrogels”, *Lab Chip* 2015, 15, 3111–3115. [PubMed: 26066320]
40. Gudapati H; Dey M; Ozbolat I, “A comprehensive review on droplet-based bioprinting: past, present and future”, *Biomaterials* 2016, 102, 20–42. [PubMed: 27318933]
41. Lee JM; Yeong WY, “Design and Printing Strategies in 3D Bioprinting of Cell-Hydrogels: A Review”, *Adv. Healthc. Mater* 2016.
42. Ozbolat IT; Hospodiuk M, “Current advances and future perspectives in extrusion-based bioprinting”, *Biomaterials* 2016, 76, 321–343. [PubMed: 26561931]
43. Mandrycky C; Wang Z; Kim K; Kim D-H, “3D bioprinting for engineering complex tissues”, *Biotechnol. Adv* 2016, 34, 422–434. [PubMed: 26724184]
44. Mironov V; Reis N; Derby B, “Review: bioprinting: a beginning”, *Tissue Eng.* 2006, 12, 631–634. [PubMed: 16674278]
45. Pati F; Gantelius J; Svahn HA, “3D bioprinting of tissue/organ models”, *Angew. Chem. Int. Ed* 2016, 55, 4650–4665.
46. Standard Terminology for Additive Manufacturing Technologies. 2012: ASTM Committee F42 on Additive Manufacturing Technologies Subcommittee F42. 91 on Terminology.
47. Bose S; Ke D; Sahasrabudhe H; Bandyopadhyay A, “Additive Manufacturing of Biomaterials”, *Prog. Mater. Sci* 2017.
48. Hockaday L; Kang K; Colangelo N; Cheung P; Duan B; Malone E; Wu J; Girardi L; Bonassar L; Lipson H, “Rapid 3D printing of anatomically accurate and mechanically heterogeneous aortic valve hydrogel scaffolds”, *Biofabrication* 2012, 4, 035005. [PubMed: 22914604]
49. Wang Z; Abdulla R; Parker B; Samanipour R; Ghosh S; Kim K, “A simple and high-resolution stereolithography-based 3D bioprinting system using visible light crosslinkable bioinks”, *Biofabrication* 2015, 7, 045009. [PubMed: 26696527]
50. Stampfl J; Baudis S; Heller C; Liska R; Neumeister A; Kling R; Ostendorf A; Spitzbart M, “Photopolymers with tunable mechanical properties processed by laser-based high-resolution stereolithography”, *J. Micromech. Microeng* 2008, 18, 125014.
51. Yamanaka Y; Yajima H; Kirita T; Shimomura H; Tamaki S; Aoki K; Yamakawa N; Imai Y, “Mandibular reconstruction with vascularised fibular osteocutaneous flaps using prefabricated stereolithographic mandibular model”, *J. Plast. Reconstr. Aesthet. Surg* 2010, 63, 1751–1753. [PubMed: 20347409]
52. Chan V; Collens MB; Jeong JH; Park K; Kong H; Bashir R, “Directed cell growth and alignment on protein-patterned 3D hydrogels with stereolithography: In this tissue engineering application, PEG-based hydrogels with different fibronectin patterns were fabricated and the influence of the protein patterns on shape and direction of seeded cells was studied”, *Virtual Phys. Prototyp* 2012, 7, 219–228.
53. Van Nunen D; Janssen L; Stubenitsky B; Han K; Muradin M, “Stereolithographic skull models in the surgical planning of fronto-supraorbital bar advancement for non-syndromic trigonocephaly”, *J. Craniomaxillofac. Surg* 2014, 42, 959–965. [PubMed: 24530077]
54. Melchels FP; Feijen J; Grijpma DW, “A review on stereolithography and its applications in biomedical engineering”, *Biomaterials* 2010, 31, 6121–6130. [PubMed: 20478613]

55. Centola M; Rainer A; Spadaccio C; De Porcellinis S; Genovese J; Trombetta M, “Combining electrospinning and fused deposition modeling for the fabrication of a hybrid vascular graft”, *Biofabrication* 2010, 2, 014102. [PubMed: 20811117]
56. Ahn S-H; Montero M; Odell D; Roundy S; Wright PK, “Anisotropic material properties of fused deposition modeling ABS”, *Rapid Prototyp. J* 2002, 8, 248–257.
57. Stevens B; Yang Y; Mohandas A; Stucker B; Nguyen KT, “A review of materials, fabrication methods, and strategies used to enhance bone regeneration in engineered bone tissues”, *J. Biomed. Mater. Res. Part B Appl. Biomater* 2008, 85, 573–582. [PubMed: 17937408]
58. Masood S; Song W, “Development of new metal/polymer materials for rapid tooling using fused deposition modelling”, *Mater. Des* 2004, 25, 587–594.
59. Naftulin JS; Kimchi EY; Cash SS, “Streamlined, inexpensive 3D printing of the brain and skull”, *PloS one* 2015, 10, e0136198. [PubMed: 26295459]
60. O’Brien CM; Holmes B; Faucett S; Zhang LG, “Three-dimensional printing of nanomaterial scaffolds for complex tissue regeneration”, *Tissue Eng. Part B Rev.* 2014, 21, 103–114. [PubMed: 25084122]
61. Castilho M; Dias M; Gbureck U; Groll J; Fernandes P; Pires I; Gouveia B; Rodrigues J; Vorndran E, “Fabrication of computationally designed scaffolds by low temperature 3D printing”, *Biofabrication* 2013, 5, 035012. [PubMed: 23887064]
62. Xu C; Chai W; Huang Y; Markwald RR, “Scaffold-free inkjet printing of three-dimensional zigzag cellular tubes”, *Biotechnol. Bioeng* 2012, 109, 3152–3160. [PubMed: 22767299]
63. Asadi-Eydivand M; Solati-Hashjin M; Shafiei SS; Mohammadi S; Hafezi M; Osman NAA, “Structure, properties, and in vitro behavior of heat-treated calcium sulfate scaffolds fabricated by 3D Printing”, *PloS one* 2016, 11, e0151216. [PubMed: 26999789]
64. Chia HN; Wu BM, “Improved resolution of 3D printed scaffolds by shrinking”, *J. Biomed. Mater. Res. Part B Appl. Biomater* 2015, 103, 1415–1423. [PubMed: 25404276]
65. Bose S; Vahabzadeh S; Bandyopadhyay A, “Bone tissue engineering using 3D printing”, *Mater. Today* 2013, 16, 496–504.
66. Farzadi A; Solati-Hashjin M; Asadi-Eydivand M; Osman NAA, “Effect of layer thickness and printing orientation on mechanical properties and dimensional accuracy of 3D printed porous samples for bone tissue engineering”, *PloS one* 2014, 9, e108252. [PubMed: 25233468]
67. Zhang X; Jiang X; Sun C, “Micro-stereolithography of polymeric and ceramic microstructures”, *Sens. Actuators A Phys.* 1999, 77, 149–156.
68. Dean D; Wallace J; Siblani A; Wang MO; Kim K; Mikos AG; Fisher JP, “Continuous digital light processing (cDLP): Highly accurate additive manufacturing of tissue engineered bone scaffolds: This paper highlights the main issues regarding the application of Continuous Digital Light Processing (cDLP) for the production of highly accurate PPF scaffolds with layers as thin as 60 μm for bone tissue engineering”, *Virtual Phys. Prototyp* 2012, 7, 13–24. [PubMed: 23066427]
69. Dean D; Mott E; Luo X; Busso M; Wang MO; Vorwald C; Siblani A; Fisher JP, “Multiple initiators and dyes for continuous Digital Light Processing (cDLP) additive manufacture of resorbable bone tissue engineering scaffolds: A new method and new material to fabricate resorbable scaffold for bone tissue engineering via continuous Digital Light Processing”, *Virtual Phys. Prototyp* 2014, 9, 3–9.
70. Hazeveld A; Slater JJH; Ren Y, “Accuracy and reproducibility of dental replica models reconstructed by different rapid prototyping techniques”, *Am. J. Orthod. Dentofacial Orthop.* 2014, 145, 108–115. [PubMed: 24373661]
71. Baldacchini T, *Three-dimensional Microfabrication Using Two-photon Polymerization: Fundamentals, Technology, and Applications.* 2015: William Andrew.
72. Zein I; Hutmacher DW; Tan KC; Teoh SH, “Fused deposition modeling of novel scaffold architectures for tissue engineering applications”, *Biomaterials* 2002, 23, 1169–1185. [PubMed: 11791921]
73. Kalita SJ; Bose S; Hosick HL; Bandyopadhyay A, “Development of controlled porosity polymer-ceramic composite scaffolds via fused deposition modeling”, *Mater. Sci. Eng. C* 2003, 23, 611–620.

74. Ning F; Cong W; Qiu J; Wei J; Wang S, “Additive manufacturing of carbon fiber reinforced thermoplastic composites using fused deposition modeling”, *Composites Part B* 2015, 80, 369–378.
75. Tan ET; Ling JM; Dinesh SK, “The feasibility of producing patient-specific acrylic cranioplasty implants with a low-cost 3D printer”, *J. Neurosurg* 2016, 124, 1531–1537. [PubMed: 26566203]
76. Espalin D; Alberto Ramirez J; Medina F; Wicker R, “Multi-material, multi-technology FDM: exploring build process variations”, *Rapid Prototyp. J* 2014, 20, 236–244.
77. Frölich A; Spallek J; Brehmer L; Buhk J-H; Krause D; Fiehler J; Kemmling A, “3D printing of intracranial aneurysms using fused deposition modeling offers highly accurate replications”, *Am. J. Neuroradiol* 2016, 37, 120–124. [PubMed: 26294648]
78. He Y; Xue G.-h.; Fu J.-z., “Fabrication of low cost soft tissue prostheses with the desktop 3D printer”, *Sci. Rep* 2014, 4.
79. Meteyer S; Xu X; Perry N; Zhao YF, “Energy and material flow analysis of binder-jetting additive manufacturing processes”, *Procedia CIRP* 2014, 15, 19–25.
80. Shirazi SFS; Gharehkhani S; Mehrali M; Yarmand H; Metselaar HSC; Kadri NA; Osman NAA, “A review on powder-based additive manufacturing for tissue engineering: selective laser sintering and inkjet 3D printing”, *Sci. Technol. Adv. Mater* 2015, 16, 033502. [PubMed: 27877783]
81. Gauvin R; Chen Y-C; Lee JW; Soman P; Zorlutuna P; Nichol JW; Bae H; Chen S; Khademhosseini A, “Microfabrication of complex porous tissue engineering scaffolds using 3D projection stereolithography”, *Biomaterials* 2012, 33, 3824–3834. [PubMed: 22365811]
82. Chen M; Le DQ; Baatrup A; Nygaard JV; Hein S; Bjerre L; Kassem M; Zou X; Bünger C, “Self-assembled composite matrix in a hierarchical 3-D scaffold for bone tissue engineering”, *Acta Biomater.* 2011, 7, 2244–2255. [PubMed: 21195810]
83. Xu T; Zhao W; Zhu J-M; Albanna MZ; Yoo JJ; Atala A, “Complex heterogeneous tissue constructs containing multiple cell types prepared by inkjet printing technology”, *Biomaterials* 2013, 34, 130–139. [PubMed: 23063369]
84. Ventola CL, “Medical applications for 3D printing: current and projected uses”, *PT* 2014, 39, 704–711.
85. Khaled SA; Burley JC; Alexander MR; Yang J; Roberts CJ, “3D printing of five-in-one dose combination polypill with defined immediate and sustained release profiles”, *J. Control. Release* 2015, 217, 308–314. [PubMed: 26390808]
86. Rees A; Powell LC; Chinga-Carrasco G; Gethin DT; Syverud K; Hill KE; Thomas DW, “3D bioprinting of carboxymethylated-periodate oxidized nanocellulose constructs for wound dressing applications”, *BioMed Res. Int* 2015, 2015.
87. Lim L-T; Auras R; Rubino M, “Processing technologies for poly (lactic acid)”, *Prog. Polym. Sci* 2008, 33, 820–852.
88. Garlotta D, “A literature review of poly (lactic acid)”, *J. Polym. Environ* 2001, 9, 63–84.
89. Serra T; Planell JA; Navarro M, “High-resolution PLA-based composite scaffolds via 3-D printing technology”, *Acta Biomater.* 2013, 9, 5521–5530. [PubMed: 23142224]
90. Narayanan G; Vernekar VN; Kuyinu EL; Laurencin CT, “Poly (lactic acid)-based biomaterials for orthopaedic regenerative engineering”, *Adv. Drug Deliv. Rev* 2016, 107, 247–276. [PubMed: 27125191]
91. Hamad K; Kaseem M; Yang H; Deri F; Ko Y, “Properties and medical applications of polylactic acid: A review”, *Express Polym. Lett* 2015, 9, 435–455.
92. Santoro M; Shah SR; Walker JL; Mikos AG, “Poly (lactic acid) nanofibrous scaffolds for tissue engineering”, *Adv. Drug Deliv. Rev* 2016, 107, 206–212. [PubMed: 27125190]
93. Weisman JA; Nicholson JC; Tappa K; Jammalamadaka U; Wilson CG; Mills DK, “Antibiotic and chemotherapeutic enhanced three-dimensional printer filaments and constructs for biomedical applications”, *Int. J. Nanomed* 2015, 10, 357.
94. Serra T; Mateos-Timoneda MA; Planell JA; Navarro M, “3D printed PLA-based scaffolds: a versatile tool in regenerative medicine”, *Organogenesis* 2013, 9, 239–244. [PubMed: 23959206]
95. Charles-Harris M; Koch MA; Navarro M; Lacroix D; Engel E; Planell JA, “A PLA/calcium phosphate degradable composite material for bone tissue engineering: an in vitro study”, *J. Mater. Sci. Mater. Med* 2008, 19, 1503–1513. [PubMed: 18266084]

96. Bidan CM; Kommareddy KP; Rumpler M; Kollmannsberger P; Fratzl P; Dunlop JW, “Geometry as a factor for tissue growth: towards shape optimization of tissue engineering scaffolds”, *Adv. Healthc. Mater* 2013, 2, 186–194. [PubMed: 23184876]
97. Kilian KA; Bugarija B; Lahn BT; Mrksich M, “Geometric cues for directing the differentiation of mesenchymal stem cells”, *Proc. Natl. Acad. Sci. U.S.A.* 2010, 107, 4872–4877. [PubMed: 20194780]
98. Almeida CR; Serra T; Oliveira MI; Planell JA; Barbosa MA; Navarro M, “Impact of 3-D printed PLA-and chitosan-based scaffolds on human monocyte/macrophage responses: unraveling the effect of 3-D structures on inflammation”, *Acta Biomater.* 2014, 10, 613–622. [PubMed: 24211731]
99. Kao C-T; Lin C-C; Chen Y-W; Yeh C-H; Fang H-Y; Shie M-Y, “Poly (dopamine) coating of 3D printed poly (lactic acid) scaffolds for bone tissue engineering”, *Mater. Sci. Eng. C* 2015, 56, 165–173.
100. Rosenzweig DH; Carelli E; Steffen T; Jarzem P; Haglund L, “3D-printed ABS and PLA scaffolds for cartilage and nucleus pulposus tissue regeneration”, *Int. J. Mol. Sci* 2015, 16, 15118–15135. [PubMed: 26151846]
101. Cui H; Zhu W; Nowicki M; Zhou X; Khademhosseini A; Zhang LG, “Hierarchical Fabrication of Engineered Vascularized Bone Biphasic Constructs via Dual 3D Bioprinting: Integrating Regional Bioactive Factors into Architectural Design”, *Adv. Healthc. Mater* 2016, 5, 2174–2181. [PubMed: 27383032]
102. Cui H; Zhu W; Holmes B; Zhang LG, “Biologically Inspired Smart Release System Based on 3D Bioprinted Perfused Scaffold for Vascularized Tissue Regeneration”, *Adv. Sci* 2016, 3.
103. Miao S; Zhu W; Castro NJ; Leng J; Zhang LG, “Four-Dimensional Printing Hierarchy Scaffolds with Highly Biocompatible Smart Polymers for Tissue Engineering Applications”, *Tissue Eng. Part C Methods* 2016, 22, 952–963. [PubMed: 28195832]
104. Singh Saharan B; Grewal A; Kumar P, “Biotechnological production of polyhydroxyalkanoates: a review on trends and latest developments”, *Chin. J. Biol* 2014, 2014.
105. Masood F; Yasin T; Hameed A, “Polyhydroxyalkanoates—what are the uses? Current challenges and perspectives”, *Crit. Rev. Biotechnol* 2015, 35, 514–521. [PubMed: 24963700]
106. Li Z; Loh XJ, “Water soluble polyhydroxyalkanoates: future materials for therapeutic applications”, *Chem. Soc. Rev* 2015, 44, 2865–2879. [PubMed: 25788317]
107. Wu J; Xue K; Li H; Sun J; Liu K, “Improvement of PHBV scaffolds with bioglass for cartilage tissue engineering”, *PloS one* 2013, 8, e71563. [PubMed: 23951190]
108. Xing Z-C; Chae W-P; Baek J-Y; Choi M-J; Jung Y; Kang I-K, “In vitro assessment of antibacterial activity and cytocompatibility of silver-containing PHBV nanofibrous scaffolds for tissue engineering”, *Biomacromolecules* 2010, 11, 1248–1253. [PubMed: 20415469]
109. Prabhakaran MP; Vatankhah E; Ramakrishna S, “Electrospun aligned PHBV/collagen nanofibers as substrates for nerve tissue engineering”, *Biotechnol. Bioeng* 2013, 110, 2775–2784. [PubMed: 23613155]
110. Masaeli E; Morshed M; Nasr-Esfahani MH; Sadri S; Hilderink J; van Apeldoorn A; van Blitterswijk CA; Moroni L, “Fabrication, characterization and cellular compatibility of poly (hydroxy alkanoate) composite nanofibrous scaffolds for nerve tissue engineering”, *PloS one* 2013, 8, e57157. [PubMed: 23468923]
111. Batchelor WM, PHA Biopolymer Filament for 3D Printing. 2016, College of William and Mary.
112. Thaxton RD, Extrusion of Polyhydroxyalkanoate Filament For Use in 3D Printers. 2016, College of William and Mary.
113. Miao S; Callow N; Zhang S; Su Z; Wang P; Liu Y, “Enzymatic synthesis of oleic acid-based epoxy monomer for the production of value added polymers”, *Biotechnol. Lett* 2013, 35, 887–890. [PubMed: 23436128]
114. Miao S; Sun L; Wang P; Liu R; Su Z; Zhang S, “Soybean oil-based polyurethane networks as candidate biomaterials: Synthesis and biocompatibility”, *Eur. J. Lipid Sci. Technol* 2012, 114, 1165–1174.
115. Miao S; Wang P; Su Z; Liu Y; Zhang S, “Soybean oil-based shape-memory polyurethanes: Synthesis and characterization”, *Eur. J. Lipid Sci. Technol* 2012, 114, 1345–1351.

116. Hong CK; Wool RP, “Development of a bio-based composite material from soybean oil and keratin fibers”, *J. Appl. Polym. Sci* 2005, 95, 1524–1538.
117. Kolanthai E; Sarkar K; Meka SRK; Madras G; Chatterjee K, “Copolyesters from soybean oil for use as resorbable biomaterials”, *ACS Sustainable Chem. Eng* 2015, 3, 880–891.
118. Sittinger M; Bujia J; Rotter N; Reitzel D; Minuth W; Burmester G, “Tissue engineering and autologous transplant formation: practical approaches with resorbable biomaterials and new cell culture techniques”, *Biomaterials* 1996, 17, 237–242. [PubMed: 8745320]
119. Shida Miao WZ; Castro NJ; Nowicki M; Zhou X; Cui H; Fisher JP; Zhang LG, “4D printing smart biomedical scaffolds with novel soybean oil epoxidized acrylate”, *Sci. Rep* 2016, 6.
120. Nishinari K; Fang Y; Guo S; Phillips G, “Soy proteins: A review on composition, aggregation and emulsification”, *Food Hydrocolloids* 2014, 39, 301–318.
121. Song F; Tang D-L; Wang X-L; Wang Y-Z, “Biodegradable soy protein isolate-based materials: a review”, *Biomacromolecules* 2011, 12, 3369–3380. [PubMed: 21910508]
122. Barkay-Olami H; Zilberman M, “Novel porous soy protein-based blend structures for biomedical applications: Microstructure, mechanical, and physical properties”, *J. Biomed. Mater. Res. Part B Appl. Biomater* 2015.
123. Koshy RR; Mary SK; Thomas S; Pothan LA, “Environment friendly green composites based on soy protein isolate—A review”, *Food Hydrocolloids* 2015, 50, 174–192.
124. Santin M; Morris C; Standen G; Nicolais L; Ambrosio L, “A new class of bioactive and biodegradable soybean-based bone fillers”, *Biomacromolecules* 2007, 8, 2706–2711. [PubMed: 17655355]
125. Chien KB; Aguado BA; Bryce PJ; Shah RN, “In vivo acute and humoral response to three-dimensional porous soy protein scaffolds”, *Acta Biomater.* 2013, 9, 8983–8990. [PubMed: 23851173]
126. Chien KB; Shah RN, “Novel soy protein scaffolds for tissue regeneration: material characterization and interaction with human mesenchymal stem cells”, *Acta Biomater.* 2012, 8, 694–703. [PubMed: 22019761]
127. Olami H; Berdicevsky I; Zilberman M, “Novel soy protein blend scaffolds loaded with antibiotics: Drug release profile bacterial inhibition effects”, *Adv. Biomater. Devices Med.* 2015, 2, 23–31.
128. Peles Z; Zilberman M, “Novel soy protein wound dressings with controlled antibiotic release: mechanical and physical properties”, *Acta Biomater.* 2012, 8, 209–217. [PubMed: 21911084]
129. Xu H; Cai S; Sellers A; Yang Y, “Intrinsically water-stable electrospun three-dimensional ultrafine fibrous soy protein scaffolds for soft tissue engineering using adipose derived mesenchymal stem cells”, *RSC Adv.* 2014, 4, 15451–15457.
130. Chien KB; Makridakis E; Shah RN, “Three-dimensional printing of soy protein scaffolds for tissue regeneration”, *Tissue Eng. Part C Methods* 2012, 19, 417–426. [PubMed: 23102234]



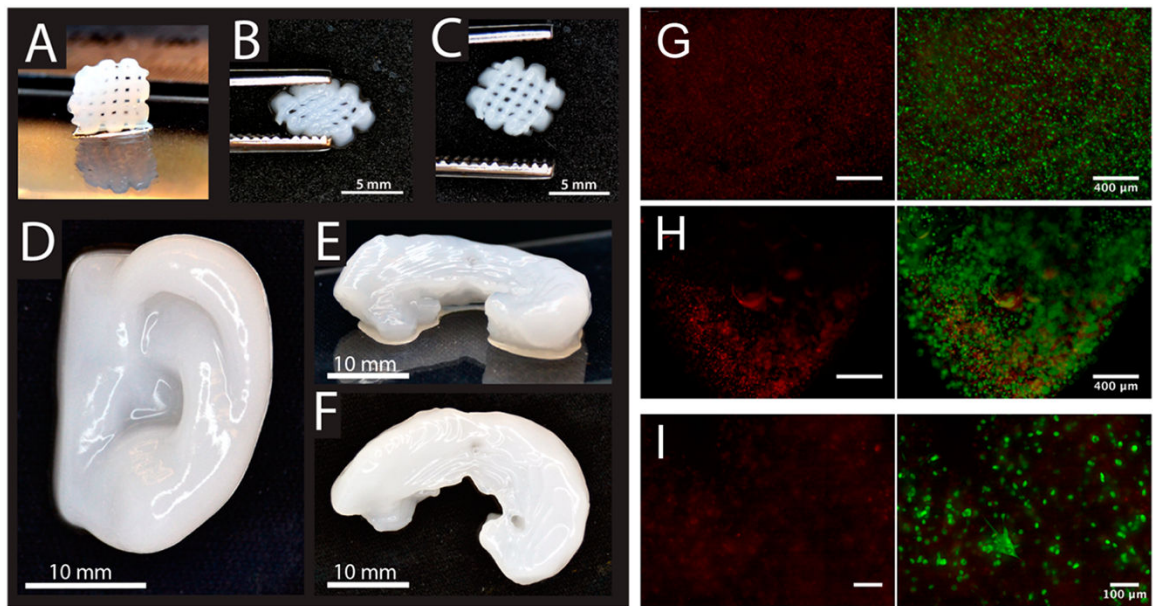


**Figure 1.**

(A) 3D printed small grids ( $7.2 \times 7.2 \text{ mm}^2$ ) with Ink8020 after cross-linking. (B) The shape of the grid deforms while squeezing, and (C) it is restored after squeezing. (D) 3D printed human ear and (E and F) sheep meniscus with Ink8020. Side view (E) and top view (F) of meniscus. (G,H) Representative images showing dead (red) and live (green) cells (G) before and (H) after bioprinting hNC in Ink8020 and 3D culture for 1 day. (I) Representative images (at  $10\times$  magnifications) showing dead and live cells in 3D printed constructs after 7 days of culture.

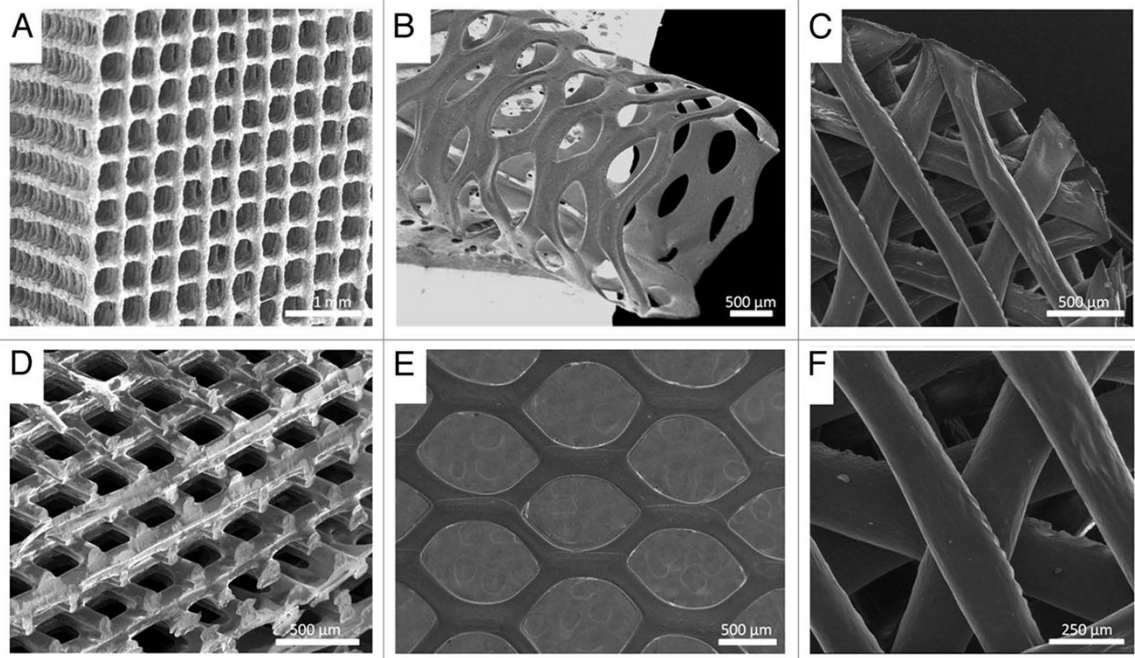


**Figure 2.** SEM images of biodegradable 3D structures with various materials, geometries and architectures, (A) PLA/CaP glass composite orthogonal structure; (B) PLA tubular hexagonal mesh; (C and F) Chitosan orthogonal-diagonal structure; (D) PLA orthogonal-displaced structure, (E) PLA hexagonal mesh.

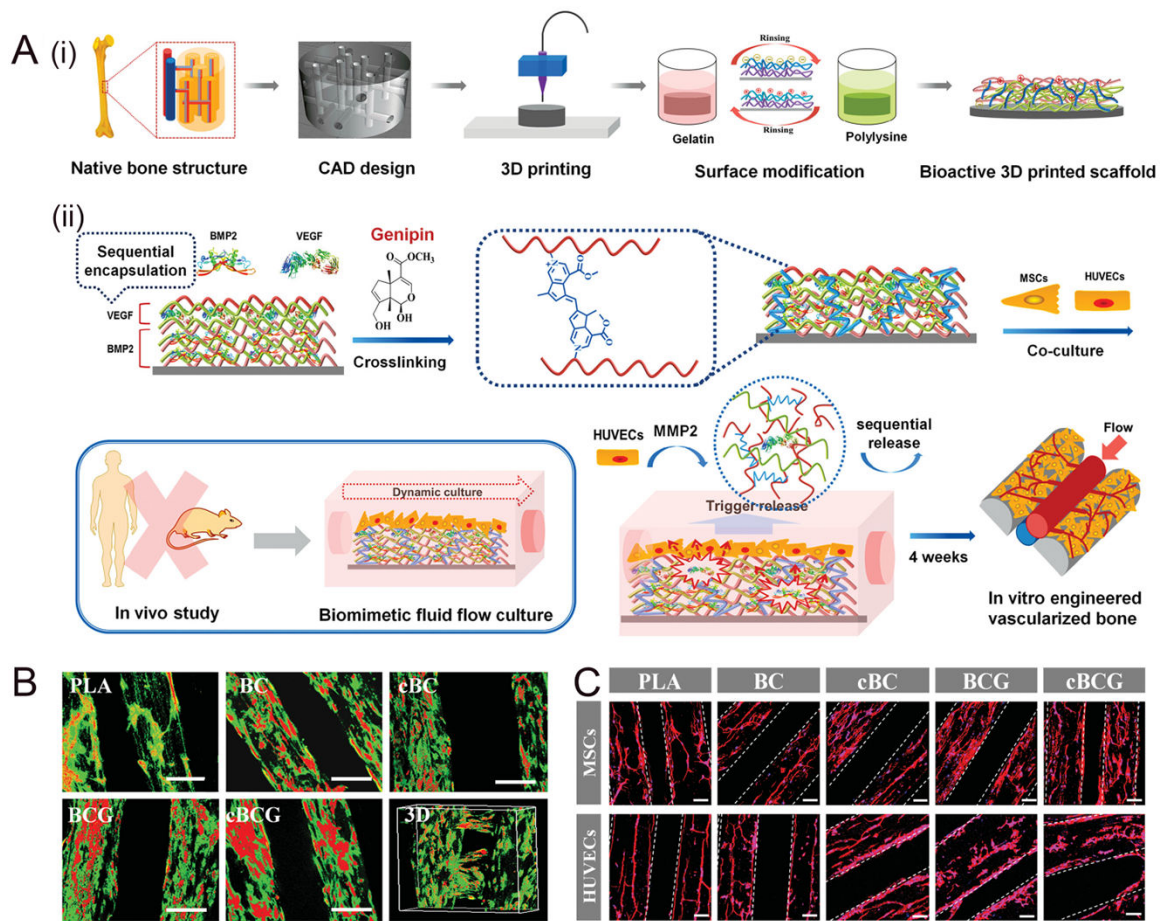


**Figure 3.**

(A) (i) Schematic illustration of the fabrication process of nanocoating modified 3D printed PLA scaffolds. According to the native bone structure, the biomimetic perfused scaffold combining bone support and vascular channels was designed and printed by FDM printer. Then surface modification process was performed to obtain a bioactive vascularized bone construct. (ii) Schematic representation of sequential adsorption and biologically inspired release of growth factors in the nanocoating film. The rhBMP-2 was adsorbed in first 15 dual-layers and then rhVEGF was adsorbed in the top 5 dual-layers together with genipin crosslinking reaction. When MSCs and HUVECs were co-cultured in dynamic fluid, the secretion of MMP2 by HUVECs could trigger the release of growth factors. After 4 weeks of culture, the vascularized bone structure would be formed *in vitro*. (B) Confocal fluorescence images of hMSCs and HUVECs co-culture on various scaffolds in a static culture condition for 5 days. hMSCs were labeled with cell tracker green, and HUVECs were stained with cell tracker red, respectively. The scale bars indicate 200  $\mu\text{m}$ . The cBCG scaffold was also imaged as 3D scanning structure. (C) Fluorescent images of hMSCs and HUVECs on the 3D printed scaffolds with F-actin (red) and nucleus (blue) staining in a static culture condition for 3 days. The hMSCs exhibited a well distributed spread on scaffold surface, while the HUVECs formed aggregative microvascular networks. The scale bars indicate 100  $\mu\text{m}$ .

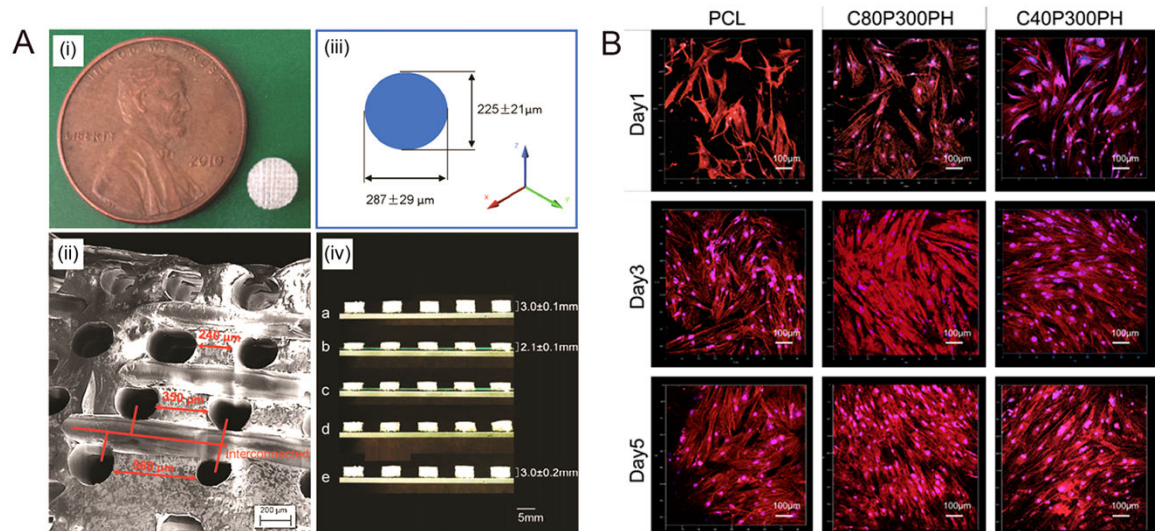


**Figure 4.**

(A) The fabricated scaffold. (i) A 5-mm-diameter and 3-mm-thickness scaffold compared to a cent. (ii) The SEM image of the pore distribution in the scaffold. (iii) Varied pore diameters in different directions. (iv) The potential for minimally invasive application; a, sample original shape; b, temporary shape at  $-18\text{ }^{\circ}\text{C}$ ; c, 0 s at  $37\text{ }^{\circ}\text{C}$ ; d, 10 s at  $37\text{ }^{\circ}\text{C}$ ; e, 3 min at  $37\text{ }^{\circ}\text{C}$ . (B) Confocal microscopy images of MSC growth and spreading morphology on printed samples of C40P300PH and C20P300PH when compared with PCL control after 1-, 3-, and 5-day culture. The color red represents cell cytoskeleton and the color blue represents cell nuclei.

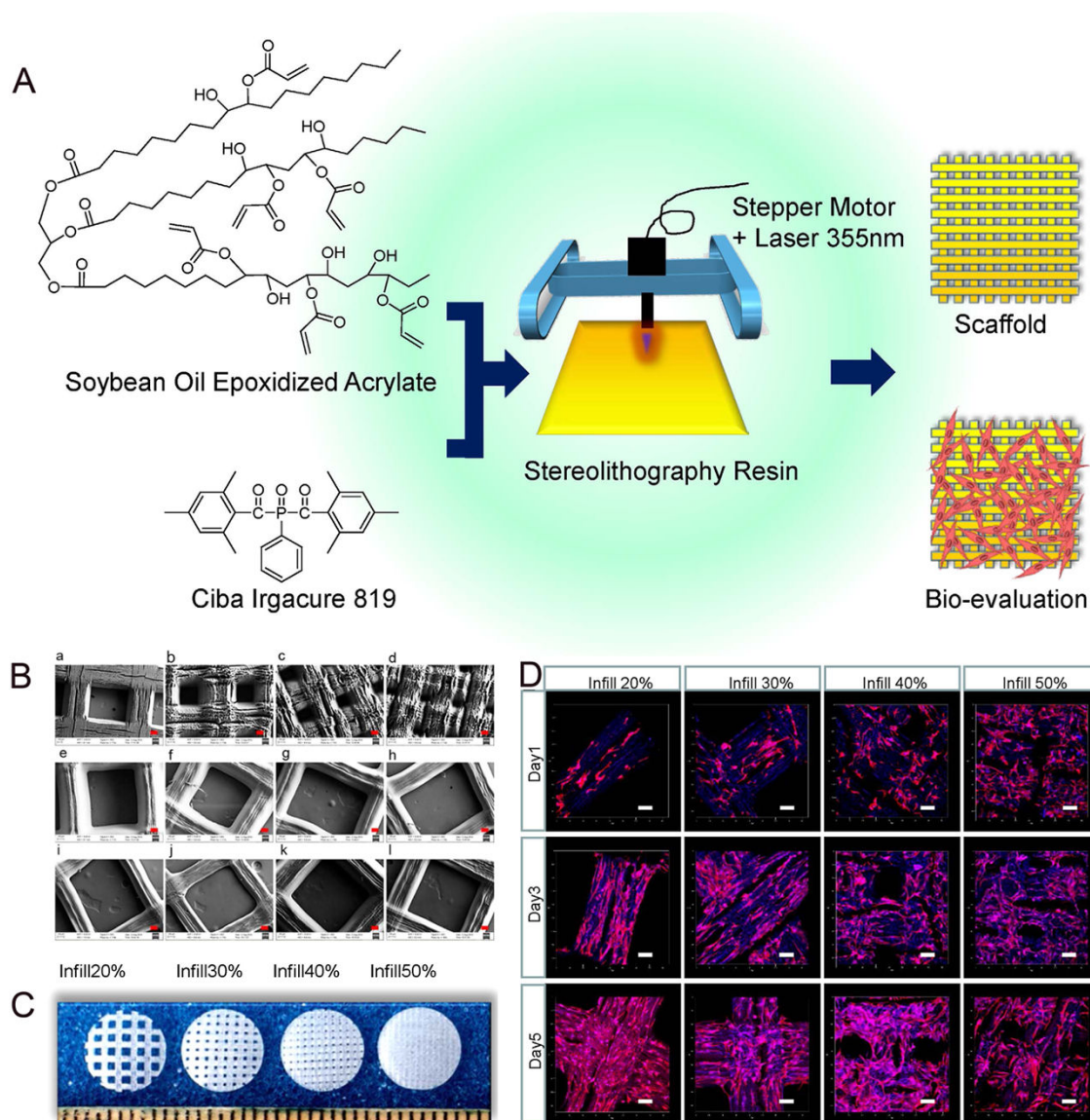


**Figure 5.**

(A) Schematic of soybean oil epoxidized acrylate fabrication process from raw material through resin fabrication and application. (B) SEM images of printed scaffolds, red scale bar 100  $\mu$  m. (a–d) Printing speed 10 mm/s, laser frequency 20000 Hz, infill density 20%, 30%, 40% and 50%, respectively; (e–j) Laser frequency 12000 Hz, infill density 20%, printing speeds 10, 20, 30, 40, 60, and 80 mm/s, respectively; (k, l) Infill density 20%, printing speed 10 mm/s, laser intensity 16000 and 8000 Hz, respectively. (C) Confocal images of hMSCs spreading on printed scaffolds from soybean oil epoxidized acrylate (printing speed 10 mm/s, laser frequency 20000 Hz) with different infill density. Data are mean  $\pm$  standard deviation, n = 6. \* p < 0.05, \*\* p < 0.01, \*\*\* p < 0.001. Scale bars are 100  $\mu$ m.

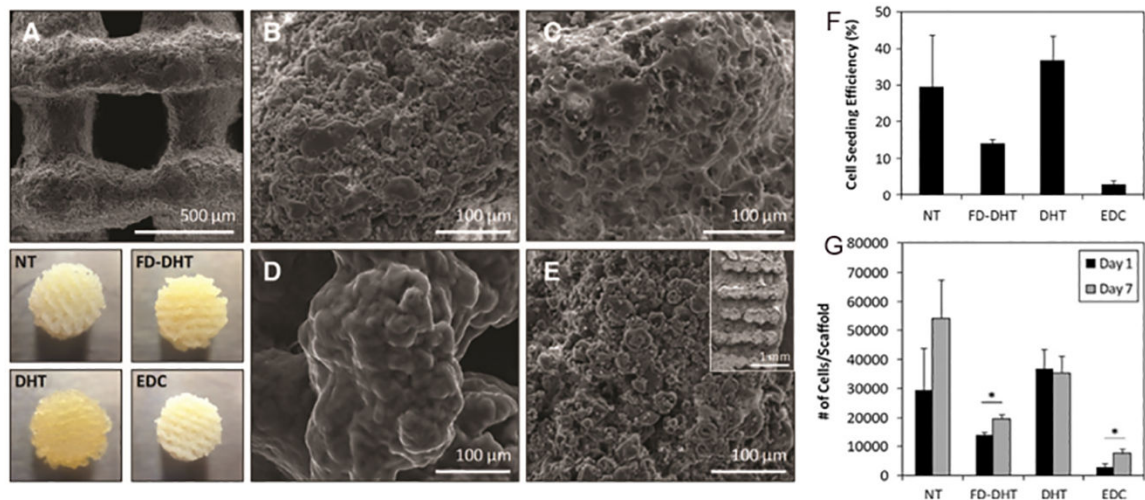


**Figure 6.**

(A-E) Effect of post-treatment on scaffold surface morphology. (A) Representative SEM image of scaffold surface showing pore structure of 90° scaffold. Below (A) are macroscopic views of 45° scaffolds with various post-treatments.  $n = 5$  for all diameters measured. Nontreated (NT): no further treatment beyond 95% ethanol dehydration. Average diameter was 6.57 – 0.19mm. Freeze-dried and dehydrothermal treated (FD-DHT): scaffolds freeze-dried before dehydrothermal treatment (DHT). Average diameter was 6.57–0.14mm. Average diameter was 4.97 – 0.33mm. 1-ethyl-3-(3 dimethylaminopropyl) carbodiimide (EDC): carbodiimide crosslinking. Average diameter was 6.09 – 0.04mm. (B–D) SEM images of the strand surface after various post-treatments. (B) NT. (C) FD-DHT. (D) DHT. (E) EDC. Inset shows representative cross sections of printed scaffolds. (F,G) Effect of post-treated scaffolds on human mesenchymal stem cell seeding efficiency and growth. (F) Cell seeding efficiency (%) of the scaffolds with starting seeding density of 100,000 cells/scaffold. (G) Proliferation of cells on scaffolds at days 1 and 7. \* $p < 0.05$ .

**Table 1:**

3D technologies and appropriate materials with advantages and disadvantages outlined

Technology	Materials	Advantages	Disadvantages
Stereolithography (vat polymerization)	Photocurable acrylate, epoxy based resins	Complex geometries, <sup>7, 48</sup> high resolution <sup>49, 50</sup>	Slow print time, <sup>51</sup> post process required (curing), <sup>52, 53</sup> limited material choice <sup>54</sup>
Fused Deposition Modelling (material extrusion)	Extrudable thermoplastics (ABS, PLA, PLGA, TPS, etc.)	strong mechanical properties, <sup>55, 56</sup> low costs, <sup>57</sup> fast printing speed <sup>58</sup>	poorer surface finish, high temperature, low resolution, <sup>59</sup> limited material choice <sup>60</sup>
Binder jetting, (powder bed and inkjet printing)	Ceramics, metals, thermoplastic polymers, composites	Fast printing speed, <sup>14</sup> complex geometries, <sup>61, 62</sup> low cost <sup>63</sup>	low resolution, <sup>64</sup> post printing process, <sup>65, 66</sup> poor mechanical properties